

AGING AND THE REDUCTION IN FRACTURE TOUGHNESS OF HUMAN DENTIN

[A. Nazari](#),¹ [D. Bajaj](#),¹ [D. Zhang](#),² [E. Romberg](#),³ and [D. Arola](#)^{1,4}.

[J Mech Behav Biomed Mater. 2009 Oct; 2\(5\): 550–559.](#)

INTRODUCTION

Advancements in medicine and an overall increase in the quality of life have resulted in far more healthy seniors in society today than in the past. By 2030 the number of Americans over 65 is expected to reach 69 million [[Bureau of the Census, 1996](#)]. That means more than 20 % of the population will be over 65, compared with only 13 % in 2006. This rise in seniors is resulting in a growing number of health care issues [[Elwood, 2007](#); [Garrett and Martini, 2007](#)]. Specifically, with the increase in lifespan there are many concerns related to mechanical properties of the hard (i.e. load-bearing) tissues and their ability to meet the physical demands over an extended period of function.

The effects of aging on the microstructure of bone and consequent reduction in the toughness of this tissue have been examined in some detail [[Currey et al., 1996](#); [Zioupos and Currey, 1998](#); [Zioupos et al., 1999](#); [Wang et al., 2002](#); [Wang and Puram, 2004](#); [Nalla et al., 2004](#); [Ural and Vashishth, 2006](#); [Ural and Vashishth, 2007](#)]. In contrast, the effects of aging on properties of dentin and enamel (i.e. hard tissues of the tooth) have received comparatively little attention. Dentin occupies the majority of the human tooth and is approximately 45 % inorganic, 30 % organic and 25 % water by volume [[Ten Cate, 1998](#)]. This tissue serves as the elastic foundation for the outermost hard and brittle enamel, as well as a protective medium for the innermost pulp. Dentin and bone have similar composition, namely both are comprised of an organic matrix of (type I) collagen fibrils, which are bound and supported by a dispersion of nanoscopic carbonated apatite crystals. Unique to dentin, it is traversed by a network of long channels (i.e. tubules) that extend outward between the pulp and the Dentin Enamel Junction (DEJ). In young dentin the tubule lumens have internal diameter of between 1 to 2 μm . But after the third decade of life there is a gradual reduction in the lumen dimensions due to a continuous deposition of mineral. After an adequate number of tubules become filled the tissue appears transparent and is then termed “sclerotic” [[Ten Cate, 1998](#)]. Detailed studies of the mineralization and crystal structure of transparent dentin have been reported and suggest that sclerosis results from dissolution and re-precipitation of minerals from the intertubular dentin within the lumens [[Nalla et al., 2005a](#); [Porter et al., 2005](#)]. As a result of the aforementioned physical changes, dentin undergoes an increase in the mineral content with aging [[Weber, 1974](#); [Vasiliadis, 1983](#)]. Interestingly, the age-related increase in mineralization of dentin contrasts with the mesoscopic reduction in mineral that takes place in cortical bone [[Thompson, 1980](#); [Currey et al., 1996](#); [Currey, 2006](#)].

Recent studies of human dentin have shown that the fracture toughness (K_{c}) ranges between 1 and 2 $\text{MPa}\cdot\text{m}^{0.5}$ and that the lowest toughness occurs in fracture perpendicular to the dentin tubules. In studies concerning this orientation, [Iwamoto and Ruse \[2003\]](#) reported that K_{c} was $1.13 \pm 0.36 \text{ MPa}\cdot\text{m}^{0.5}$, whereas [Imbeni et al., \[2003\]](#) reported a K_{c} of $1.79 \pm 0.05 \text{ MPa}\cdot\text{m}^{0.5}$; neither investigation addressed the potential importance of patient age. [Kinney et al. \[2005\]](#) examined properties of sclerotic dentin and reported that the fracture toughness ($1.46 \pm 0.11 \text{ MPa}\cdot\text{m}^{0.5}$) was substantially lower than that of young “normal” tissue. Similarly, a recent evaluation [[Koester et al., 2008](#)] showed that the growth toughness¹ of aged dentin ($40 \leq \text{age} \leq 70$) is significantly lower than that of younger tissue. *In situ* observations of crack growth showed that filling of the lumens with mineral

suppressed the primary mechanisms of extrinsic toughening that were active in the young tissue. That study provided fundamental information concerning properties and mechanisms, but evaluated cracks in the plane of the tubules and over a limited degree of extension ($\Delta a \leq 250 \mu\text{m}$). The most common orientation of cracks and fracture surfaces in the coronal dentin of human teeth is perpendicular to the tubules [Arola et al., 2002; Arola, 2007; Bajaj et al., 2008]. As such, an understanding of the age-related reduction in crack growth resistance of this orientation is most relevant, but currently lacking.

The primary objectives of this investigation were to quantify the fracture toughness of human dentin for cracks extending perpendicular to the dentin tubules and to characterize the influence of patient age on the crack growth resistance. The evaluation examines the responses over clinically relevant flaw lengths ($\Delta a \leq 1 \text{ mm}$) and correlates the age-dependent mechanical behavior with the changes in microstructure.

MATERIALS AND METHODS

Human third molars of patients between ages 18 and 83 were obtained from dental clinics in Maryland in compliance with the Institutional Review Board of the University of Maryland Baltimore County. All teeth were obtained from living patients and the teeth were inspected to insure that they were free of damage or demineralization (i.e. caries free). Selected teeth ($N=14$) were divided by patient age into young ($18 \leq \text{age} \leq 35$), middle and old ($55 \leq \text{age}$) groups according to a previous study [Bajaj et al., 2006]. A single Compact Tension (CT) specimen (Fig. 1(a)) was sectioned from the coronal dentin of each tooth using a slicer/grinder with diamond abrasive wheels. Note that the specimens were sectioned such that the tubules were perpendicular to the direction of crack growth and the plane of fracture. The methods and equipment used in preparing specimens have been described elsewhere [Bajaj et al., 2006; Zhang et al., 2007] and a detailed view of the specimen geometry is shown in Figure 1(b). Due to the precision of the equipment used in manufacturing specimens the geometry was within $25 \mu\text{m}$ of the target dimensions. In addition, assuming a yield strength of 110 MPa [Arola and Reprogel, 2005; Arola and Reprogel, 2006] and fracture toughness of roughly $1.8 \text{ MPa}\cdot\text{m}^{0.5}$ [Imbeni et al., 2003], the geometry achieves plane strain conditions [Anderson, 2004].

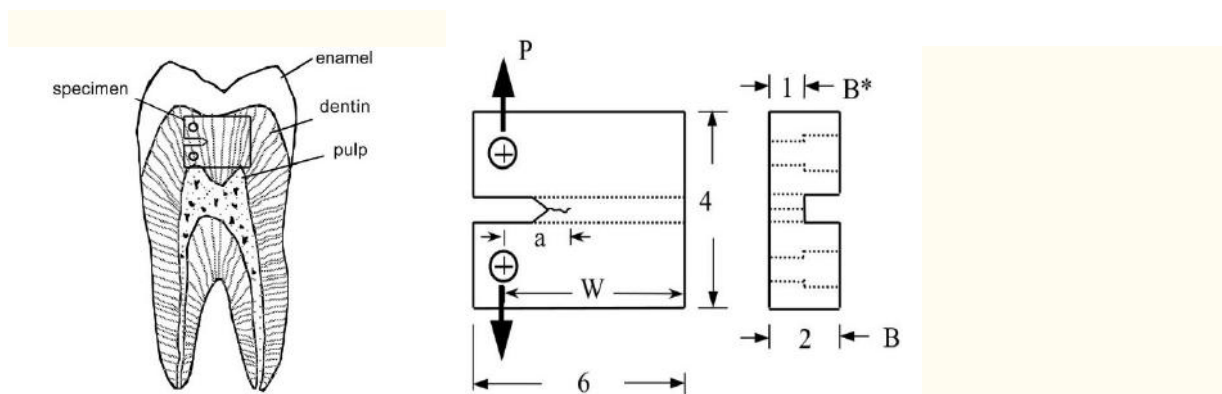


Figure 1

Schematic diagrams describing the development of specimens for evaluating the fracture resistance of human dentin.

a) a schematic diagram of a sectioned molar with an outline of a potential specimen that could be prepared. Note that the faint gray lines in the dentin distinguish the course of the dentin tubules extending from the pulp. The lines distinguish direction but not the tubule density.

b) the compact tension specimen geometry. Note that according to the nature of preparation shown in (a), the dentin tubules are oriented parallel to the direction of loading. A single specimen was prepared from each tooth.

Each of the CT specimens was subjected to cyclic loading to initiate a well-defined pre-crack at the tip of the machined notch root (Fig. 1(b)). Cyclic loading was achieved using an Enduratec Model 3200 universal testing system and employed a stress ratio (R) of 0.5, frequency of 5 Hz and a maximum load of between 5 to 10 Newtons. According to the work of Imbeni et al [2003], a pre-crack was considered essential to obtain accurate estimates of toughness for dentin. Yet, the pre-cracks were grown less than 0.5 mm from the notch tip to limit the development of potential features that would contribute to extrinsic toughening at the onset of stable crack extension. Quasi-static Mode I loading of the specimens was then performed using a specially designed computer controlled universal loading frame complemented with a microscopic imaging system consisting of a stereo light microscope² with optical output, a progressive scan CCD camera³ and an imaging board [Zhang et al., 2006]. Quasi-static loading was performed incrementally under load control actuation until the onset of crack growth. Thereafter, loading was continued in displacement control to achieve increments of stable crack extension. The specimen was partially unloaded by approximately 0.25 N after each increment, and then reloaded to continue the extension. A load vs. load-line displacement response highlighting the pre-loading (Region I) and incremental stable crack extension (Region II) portions of testing is shown for a selected specimen in Figure 2(a). Digital images were acquired using the stereomicroscope at the onset of each loading increment, at the peak load, and immediately following extension to fully document the crack growth process. The procedures were continued in this manner until the specimen fractured. Note that the specimens were maintained moist with HBSS (23 °C) throughout the pre-crack and monotonic loading phases of evaluation.

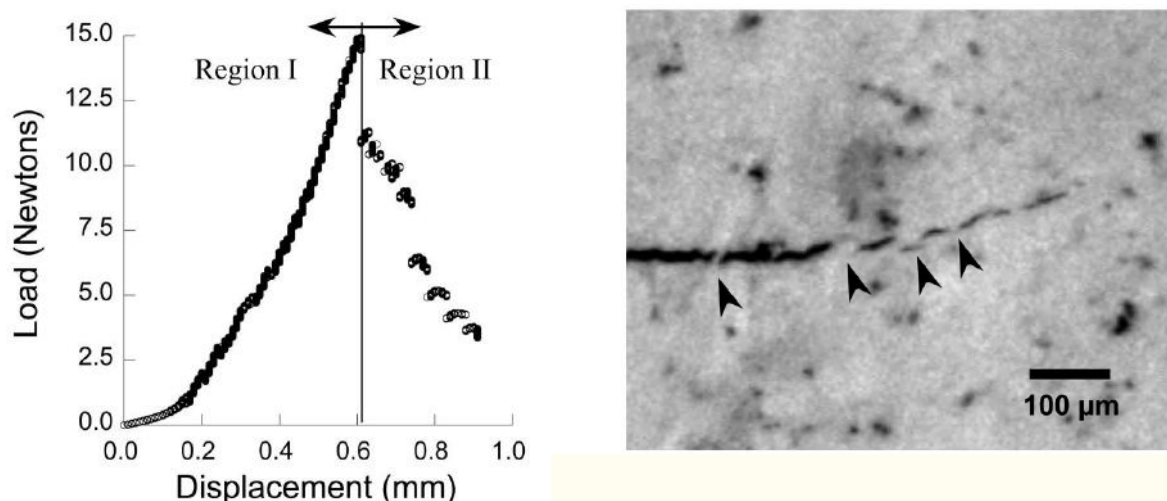


Figure 2

Details of the experimental evaluation including quasi-static loading of the dentin specimens and methods for documenting crack extension.

a) a load load-line displacement distribution obtained during stable crack extension within a dentin specimen. Region II distinguishes the portion of response associated with incremental stable crack extension.

b) a digital image of a stable crack in a dentin specimen and the “speckle” distribution used in the DIC analysis. Note the unbroken ligaments of dentin located behind the crack tip and highlighted by the black arrows.

The full-field displacement distribution and the crack length measurements were obtained by performing Digital Image Correlation (DIC) with the acquired microscopic images. Prior to quasi-static loading, the dentin specimens were coated with a very thin layer (approximately 5 µm) of diluted correction fluid mixed with toner powder (Fig. 2(b)). The coating provided a distribution of fine black speckles on a white background and

facilitated the correlation process [Zhang and Arola, 2004; Zhang et al., 2006]. In general, DIC is comprised of comparing a digital image of the CT specimens in the undeformed state (before loading) with images obtained in the deformed state (under load). The comparison was conducted over the entire field of view using sequential subsets of pixels over the digitized space. Using the digital microscopic images and subpixel correlation techniques [Zhang et al., 2006] a displacement resolution exceeding 0.1 μm was achieved. The correlation process provided the displacements in the directions parallel (u) and perpendicular (v) to the direction of crack extension over the entire field of view. The displacement fields were used to examine the crack opening displacement (COD) profile over the entire extension history. In turn, the COD distributions were used to precisely identify the crack tip from the location of zero opening displacement (i.e. the vertex of the COD distribution at $v = 0$).

Using the load and crack length measurements, the mode I stress intensity distribution (K_I) in the CT specimens was estimated according to [Bajaj et al., 2006]

$$K_I = P B^* W^{-1/2} \sqrt{(B^* + 1) B + 1} \left[0.131 + 0.320 \alpha + 0.211 \alpha^2 \right] \left[\text{MPa} \cdot \text{m}^{0.5} \right] \quad (1.4 \leq a \leq 3.0) \quad (3)$$

where P is the opening load (Newtons), α is the ratio of a to W (Fig. 1(b)) and the quantities B^* and B (mm) are the reduced thickness (within the region of the channel) and nominal specimen thickness, respectively. Equation 3 is valid for $1.4 \leq a \leq 3.0$ mm [Bajaj et al., 2006] where the crack length (a) represents the sum of the physical crack length (grown from the notch tip) and the machined notch precursor to the center of the load line as illustrated in Figure 1(b). Note that the K_I distribution defined by this equation provides the average stress intensity across the specimen's thickness. The critical stress intensity was then evaluated in terms of the incremental crack extension to examine the crack growth resistance history (i.e. R-curve) for each specimen. The R-curves were then pooled in terms of the patient age and further analysis was performed to identify significant differences in the degree and nature of toughening.

The fractured CT specimens were dehydrated in air for approximately 24 hours, sputtered with gold palladium, and then examined using a Jeol JSM 5600 scanning electron microscope (SEM) in the secondary electron imaging mode. The average lumen diameter and ratio of the average lumen and peritubular cuff areas were estimated from images of the microstructure. Briefly, Backscatter Electron Imaging (BEI) mode was used to differentiate between the lumen, peritubular cuff and the surrounding intertubular dentin. A complementary quantitative description of the microstructure was obtained from an image analysis and summation of pixels corresponding to the lumens and distinct constituents [Arola, 2007]. Statistical differences in the crack growth resistance and the dentin tubule geometry with age were calculated using an ANOVA with Tukey's HSD; significance was defined by $p < 0.05$. Correlations between age and the crack growth resistance were evaluated using Pearson's r.

RESULTS

A typical crack growth resistance curve for young dentin is shown in Figure 3(a) and documents nearly 1 mm of stable extension beyond the existing fatigue crack. Most of the young dentin specimens underwent at least 1 mm of controlled extension, which exceeded that obtained in the older group. Stable crack growth was comparatively difficult to achieve in the old dentin. In general, most of the dentin specimens exhibited a rise in the stress intensity necessary to continue stable crack growth (i.e. rising R-curve); the degree of rise in critical stress intensity with crack extension decreased with patient age. Based on the distinct toughening behavior, the responses were conveniently quantified in terms of the initiation (Region I) and growth (Region II) responses evident in Figure 2(a).

Specifically, the magnitude of stress intensity at the onset of stable crack extension from the existing fatigue crack was quantified in terms of the “initiation toughness” (K_o) as denoted in [Figure 3\(a\)](#). Similarly the “plateau toughness” (K_p) was used to define the maximum crack growth resistance as evident from the plateau in growth response. The K_p is also regarded here as the maximum toughness (i.e. fracture toughness: K_c). The rise in resistance with incremental extension between K_o and K_p was quantified by the slope of the stress intensity distribution and is termed the “growth toughness” (K_g).

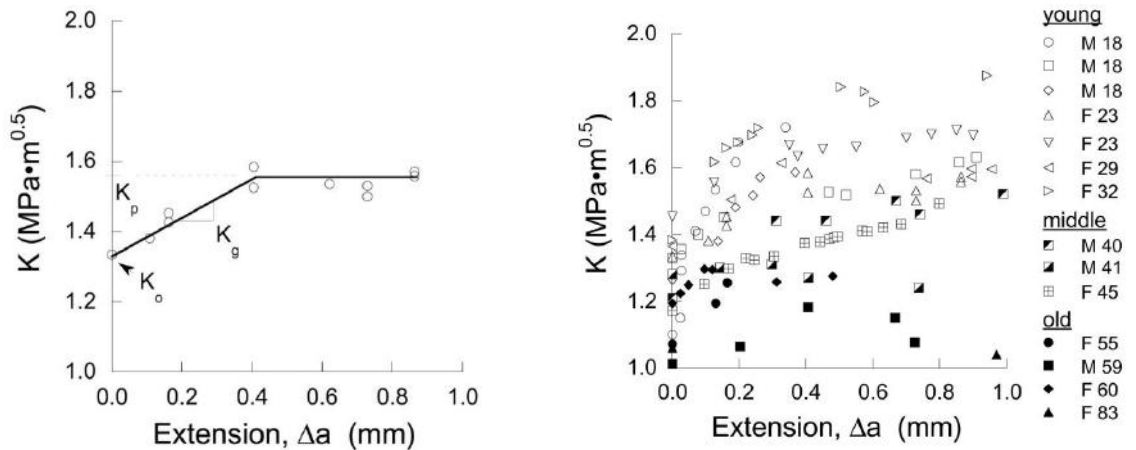


Figure 3

Crack growth resistance (R-curve) responses for the dentin specimens.

- a typical resistance curve for young dentin and identification of the components of toughness. This R-curve was obtained for stable crack extension within dentin from a 23 year old female.
- results from all of the specimens. The gender and age are listed for each of the specimens.

Crack growth resistance curves for all the dentin specimens are shown in [Figure 3\(b\)](#) including results for the three age groups. Stable crack extension initiated at a stress intensity of $1 \text{ MPa}\cdot\text{m}^{0.5}$ or greater in all samples. There is a noticeable reduction in the degree of toughening achieved with increasing patient age. Results of the quantitative estimates for initiation, growth and plateau toughness are listed in [Table 1](#). According to the average responses, there was nearly a 20% difference in the K_o and 30% difference in K_p between the young and old dentin. The differences in the K_o and K_p between the young, middle and old dentin groups were significant ($p < 0.0001$). Although there was a reduction in the magnitude of K_g with age overall, there was no significant difference in this component of toughening obtained between any of the three age groups.

Table 1

A comparison of the crack growth resistance for the three age groups. All data is presented in terms of the mean and (std dev) for results of all specimens in the group.

Crack Growth Resistance	Young	Middle	Old	p^*
Initiation, K_o ($\text{MPa}\cdot\text{m}^{0.5}$)	1.34 (0.06) ^a	1.22 (0.06) ^b	1.08 (0.08) ^c	0.0001
Growth, K_g ($\text{MPa}\cdot\text{m}^{0.5}/\text{mm}$)	0.93 (0.39) ^a	0.22 (0.15) ^a	0.64 (0.52) ^a	NS
Plateau, K_p ($\text{MPa}\cdot\text{m}^{0.5}$)	1.65 (0.10) ^a	1.43 (0.10) ^b	1.17 (0.09) ^c	0.0001

Note: Statistical significance is indicated by superscripts (a, b, c) and p-values. NS indicates not significant. $p \leq 0.0001$ and $p \leq 0.05$ are also indicated for comparisons between groups.

*groups with the same letter are not significantly different

NS = not significant

The three components of toughness are presented in terms of the total patient age spectrum in [Figure 4](#). Results in [Figure 4\(a\)](#) show that there was a distinct and nearly uniform reduction in the K_o with age. Using a linear least-squares error description for the distribution, there is a reduction in the initiation toughness of approximately 5 % per decade. Though there appears to be a reduction in the apparent growth toughness with age ([Fig. 4\(b\)](#)), there was no definite trend in the data as indicated by the degree of correlation. However, similar to K_o there was a uniform reduction in the K_p with patient age ([Fig. 4\(c\)](#)). A linear trend approximation of the changes in K_p indicates that there is a reduction of at least 5 % per decade. According to the estimates of Pearson's r , the correlations between age and K_o ($r = -0.81$) as well as age and K_p ($r = -0.87$) were both highly significant ($p < 0.0001$).

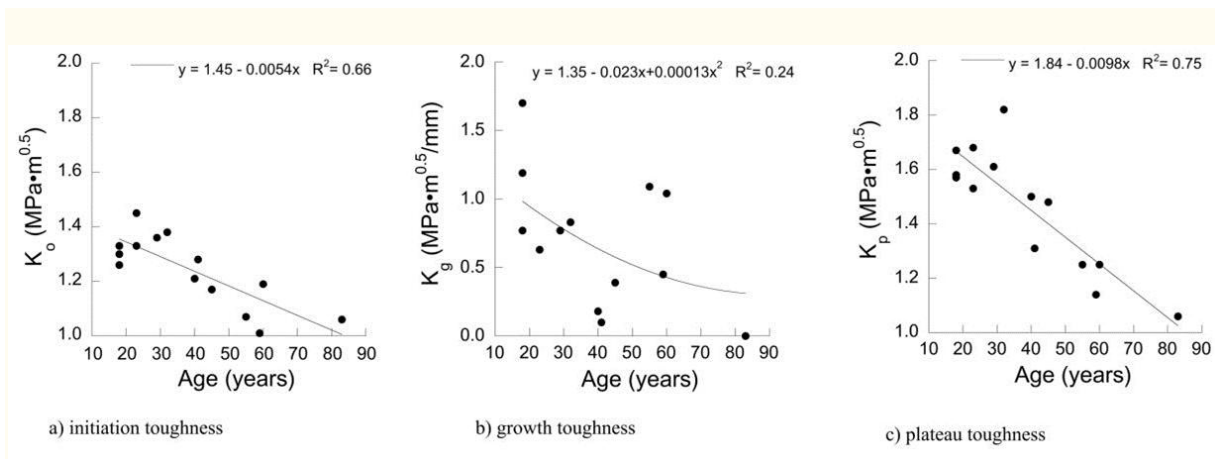


[Figure 4](#)

The decrease in individual components of fracture toughness with patient age.

Observations of the crack growth process revealed that unbroken ligaments of dentin developed during extension and operated behind the advancing crack (e.g. [Fig. 2\(b\)](#)) in promoting extrinsic toughening via posterior closure forces. These ligaments were frequently identified in the young specimens but seldom noted in specimens of the old group. On the macroscopic level the fracture surfaces of the three age groups appeared very similar. Yet, on the microscopic level there were distinct differences, and most notably in characteristics of the fractured peritubular cuffs. Micrographs obtained from the fracture surfaces are shown in [Figure 5](#). In fracture surfaces of young dentin ([Fig. 5\(a\)](#)) the peritubular cuffs were located below the primary plane of fracture or with respect to the surrounding intertubular dentin. Also, many of the cuffs were cracked or exhibited multiple radial microcracks about the circumference as highlighted in [Figure 5\(a\)](#). Some of the cuffs were partially separated from the surrounding mineralized matrix, suggesting that the tubules underwent debonding or suffered from a loss of cohesion. In the old dentin ([Fig. 5\(b\)](#)) there was little difference between the plane of fracture of the intertubular and peritubular components, which resulted in a more uniform (or smooth) surface height distribution. In contrast to the microstructural damage in young dentin, there was minimal evidence of microcracking or radial fractures of the old peritubular cuffs. While these features are not evident in [Figure 5\(b\)](#), microcracks were occasionally identified in the peritubular components of old dentin and were limited to those with tubules that were not completely filled with mineral. It is worthwhile noting that the observations were made using a conventional SEM. As such, partial dehydration of the samples occurs during the required sputtering process and the SEM analysis, which could introduce artifacts in the fracture surfaces (i.e. microcracks). Nevertheless, there were no

constraints imposed to the shrinkage, which enabled free volumetric contraction, thereby inhibiting the potential development of microcracks.

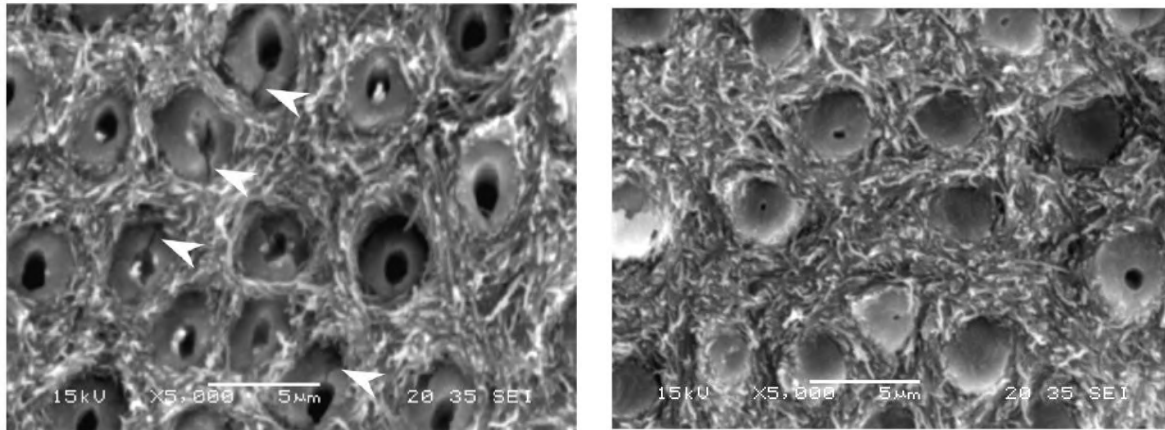


Figure 5

Scanning electron micrographs of the fracture surfaces. Crack extension occurred from left to right for both of the specimens.

a) young dentin (24 year old male). Note the fractured peritubular cuffs highlighted by the white arrows. Also note the recession of the peritubular cuffs with respect to the plane of the surrounding intertubular dentin.

b) old dentin (76 year old female). Note the absence of fractured cuffs in comparison to young dentin in (a), as well as the consistency in fracture surface of the intertubular and peritubular components.

Perhaps the most notable difference between the fracture surfaces of the young and old dentin in [Figure 5](#) is the extent of mineral filling the lumens; the diameter of the lumens decreased with age. A quantitative description of the microstructure in terms of the area ratios of the lumen (L) and peritubular cuff (C) is presented in [Figure 6](#) for the three age groups. There was a significantly larger degree of mineral filling the lumens of old dentin than in both the young ($p < 0.0001$) and middle aged ($p < 0.05$) tissue. It is important to highlight that the number of filled lumens and degree of filling was not constant over the fracture surfaces and that the measures in [Figure 6](#) represent an average of the tubule dimensions over approximately 5 different locations. Equally important, some of the older teeth exhibited regions of transparency, and particularly near the root apex. While there were some areas of transparent dentin in the crown regions of the old teeth, none of the teeth were comprised entirely of transparent tissue. Therefore, quantification of the transparency within the CT specimens would be far more subjective than the lumen measurements ([Fig. 6](#)) and was not characterized.

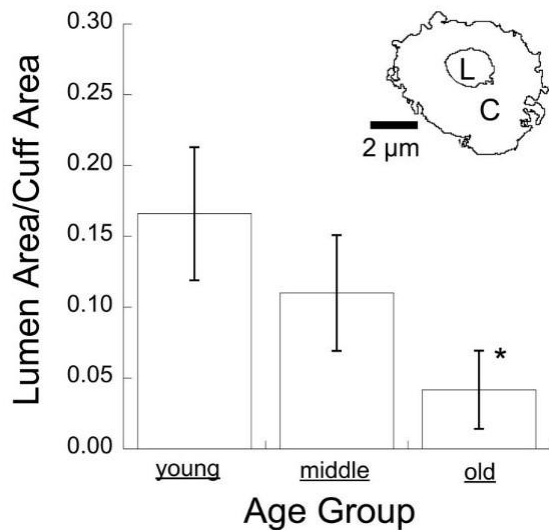


Figure 6

Average tubule dimensions for the three age groups evaluated. The inset shows a wire frame outline of a single dentin tubule obtained using backscatter electron imaging and further processing; the letters L and C distinguish the lumen area and cuff area of the image, respectively.

* The ratio of lumen to cuff area of the old dentin is significantly lower than that of the young ($p < 0.0001$) and middle ($p < 0.05$) age groups.

DISCUSSION

Results of this experimental evaluation showed that there is a significant reduction in the crack growth resistance of human dentin with increasing age, which confirm the findings of recent studies on aged and sclerotic dentin [Kinney et al., 2005; Koester et al., 2008]. They are also in agreement with studies on the fatigue behavior, which have reported that there is a significant decrease in the fatigue strength of human dentin and the resistance to cyclic crack growth with patient age [Arola and Repegel, 2005; Kinney et al., 2005; Bajaj et al., 2006; Bajaj et al., 2008]. But there are unique findings and important differences from these earlier studies that are essential to highlight.

A comparison of results for the three age groups (Table 1) revealed that the average fracture toughness (i.e. $K_c = K_p$) of the old dentin was approximately 30 % lower than that of young dentin. Kinney et al. [2005] reported that the fracture toughness of sclerotic dentin ($1.46 \text{ MPa}\cdot\text{m}^{0.5}$) was only 20 % lower than that of normal tissue ($1.79 \text{ MPa}\cdot\text{m}^{0.5}$). That study was conducted with specimens comprised of coronal and radicular dentin, which possess distinctly different tubule dimensions and densities [Mjor and Nordahl, 1996; Schilke et al., 2000]. In examination of the toughening behavior, the average growth toughness of the old dentin (Table 1) in the present study was approximately 30 % lower than that of the young group. Koester et al. [2008] found that K_g of old dentin was approximately 40 % lower than that of young dentin (ranging from 30 % to 60 %) and depended on the degree of sclerosis. That evaluation also included specimens of coronal and radicular dentin, but concentrated on cracks extending within the plane of the tubules, perpendicular to the direction studied here. Collectively these studies distinguish that regardless of the region of the tooth evaluated and orientation of crack extension, there is a significant decrease in the crack growth resistance of dentin with age. But the extent of reduction appears dependent on the tubule density, which is important to the mineral to collagen ratio and the regional variation in the degree of changes to this ratio with aging and sclerosis. Though sclerosis begins in the root apices and progresses coronally [e.g. Carrigan et al., 1984], differences in the initiation of sclerosis and the rate at which mineral fills the tubules in the root and crown have not been described in detail. These factors are expected to cause regional differences in the apparent reduction of the crack growth resistance with aging and are reserved for future study.

Tubule orientation may play the largest role on the extent of reduction in crack growth resistance with age due to differences in, and relative potency of, the primary mechanisms of toughening. One important aspect of the R-curves in Figure 3 is that the rise in toughness with crack extension (i.e. quantified by K_p/K_o) ranges from approximately 1.2 to 1.7 for the young dentin (average = 1.3). For tissue of the same age group the rise in

toughness for crack growth occurring in plane with the tubules ranged between a factor 2 and 3 [Koester et al., 2008]. And in similar evaluations on human bone the increase in toughness reportedly ranges from 2 to nearly 5 [e.g. Malik et al., 2003; Nalla et al., 2005b]. The toughening that accompanies crack growth perpendicular to the dentin tubules is the lowest of these mineralized tissues overall, and provides some understanding towards why the majority of tooth fractures in the crown of teeth are oriented perpendicular to the tubules [Arola et al., 2002; Arola, 2007; Bajaj et al., 2008]. It is clear that the R-curve behavior of human dentin is orientation dependent, but it is not clear how aging affects anisotropy in the crack growth resistance behavior. A study of the transition from stress-life fatigue to cyclic crack growth in dentin distinguished that the degree of anisotropy⁴ in fracture resistance under cyclic loading decreases with increasing crack length from approximately 2 (for short cracks) to 1.2 (for long cracks) [Arola et al., 2007]. The individual measures for K_p (Fig. 4(c)) provided estimates for average toughness that reduced from 1.65 for young dentin to 1.17 (Table 1), whereas estimates for crack extension parallel to the tubules from data in [Koester et al., 2008] provides values for the two ages of roughly 2.1 and 1.5. Using these values to quantify the degree of anisotropy for young and old dentin ($K_c(\theta=0^\circ)/K_c(\theta=90^\circ)$) provides an average near 1.3 for both age groups (i.e. over the entire age spectrum). It is important to note that the aforementioned estimates were obtained from a relatively limited data set. Nevertheless, these findings suggest that: 1) the degree of toughening with crack extension is lowest for cracks extending perpendicular to the tubules, regardless of age, and 2) while the toughness of dentin decreases with age, the degree of anisotropy in resistance to fracture does not. That is of tremendous clinical relevance and requires further validation.

There were significant reductions in the initiation and plateau toughness (Fig. 4) with age that undoubtedly result from degradation in the mechanisms of toughening. The rise in crack growth resistance signifies the contribution of extrinsic mechanisms of toughening that operate behind the crack and reduce the local near-tip stress intensity. Extrinsic toughening originated from unbroken ligaments of tissue (e.g. Fig. 2(b)) operating in the wake up to approximately 500 μm behind the crack tip, as well as collagen fibrils that spanned the crack faces over tens of micrometers behind the tip (not shown). Both of these contributions have been documented in previous studies of the crack growth behavior of elephant [Nalla et al., 2003; Kruzic et al., 2003] and bovine [Kahler et al., 2003] dentin. Evident in young dentin, the ligaments developed from microcracking and fracture of the peritubular cuffs in the K-dominant region ahead of the crack tip. Observations of the samples using the SEM distinguished these characteristics in the fracture surface of the young dentin samples (Fig. 5(a)). Similar observations were made for cracks propagating in plane with the dentin tubules during in situ experiments [Koester et al., 2008]. There, microcracked tubules reportedly served as the catalyst for crack deflection and crack branching. Neither of these mechanisms were noted here, which simply reinforces that the orientation dependence in crack growth resistance is a result of differences in the toughening mechanisms. They are also certainly age dependent. The microstructural changes with aging (Fig. 6) suppressed the contribution of microcracking to the crack growth resistance. Tubules filled with mineral would appear to be more resistant to fracture due to the increase in effective cross-section, and therefore become less- or in-capable of facilitating the development of unbroken ligaments. Indeed, there were few or no unbroken ligaments identified in the crack wake during testing performed on the old specimens. There was also comparatively little or no evidence of collagen fibril bridging. In turn, cracks in the old dentin propagated primarily by development of a critical stress intensity at the crack tip, rather than by the incubation of cracked or damaged material within the K-dominant region and progression of the crack by linking of these regions. Since the unbroken ligaments are believed to have initiated at microcracked tubules, the significant difference in K_p between the young and old dentin (Fig. 4(c)) appears to be primarily attributed to the mineral filling the lumens.

Though the largest reduction in crack growth resistance with age was exhibited by the K_{Ic} (Fig. 4(c)), there was also a significant ($p < 0.0001$) reduction in the initiation toughness (K_{I0}) with age (Fig. 4(a)). That observation is unique from previously reported studies and highlights that aging of dentin is accompanied by a reduction in the intrinsic toughness. The reduction in K_{I0} could be attributed to an increase in the mineral content of the intertubular dentin. That would promote embrittlement of the mineralized matrix and an increase in the flaw sensitivity, thereby reducing the energy required for the development of new crack area. But the comment is speculative. Although there is an increase in the mineral content of dentin with age overall, no differences have been identified in the mineral content of intertubular dentin between young and old teeth [Weber, 1974; Vasiliadis et al., 1983]. An equally relevant but far less discussed contribution could arise from a reduction in the collagen content or a change in the constitutive behavior of the collagen fibrils that reduces the toughness of the intertubular dentin. There was evidence that the collagen played an important role on the fracture process in young dentin through inelastic deformation of the intertubular matrix. Recession of the peritubular cuffs on the fracture surfaces of young dentin shown in Figure 5(a) could result from fracture and pullout, much like that in fiber reinforced composites. But all of the peritubular cuffs existed below the plane of fracture (Fig. 5(a)); there were essentially no cuffs extending above the global fracture surface. The most plausible explanation is that the mineralized collagen matrix undergoes local inelastic deformation, which provides further resistance to crack extension beyond failure of the tubules and facilitates blunting. By virtue of the fractured surface features (Fig. 5(b)), old dentin loses the capacity for this inelastic deformation, an observation made earlier from the load displacement response of transparent dentin [Kinney et al 2005] and constitutive behavior of old dentin [Arola and Reprogel, 2005] in flexure. Either the collagen fibrils lose their extensibility and toughness, or the collagen content has decreased, thereby increasing the mineral to collagen ratio and apparent brittleness.

There is presently limited understanding of the changes to the collagen matrix in dentin with aging. An evaluation of dentin using Deep UV resonance Raman spectroscopy showed that there was an increase in the amide I peak height of the dentin collagen with patient age [Ager et al., 2006]. The rise in peak intensity was not believed to arise from changes in the fibrils themselves. Rather, an increase in packing density of the mineral crystallites about the collagen fibrils and/or changes to local stresses in the fibrils due to dehydration were considered responsible. An earlier study [Walters and Eyre, 1983] noted that the number of hydroxypyridinium crosslinks in human dentin increased with patient age, but that the total number of cross-linking bonds per collagen molecule decreased by approximately 25% over a period of 40 years (from age 15 to 56). That would suggest that the reduction in resistance to fracture is due to a reduction in degree of cross-linking. Indeed, an increase in intermolecular hydrogen bonding of the collagen fibrils resulting from chemical dehydration of dentin by polar solvents has been shown capable of increasing the crack growth resistance of dentin [Nalla et al., 2006]. But it is important to note that the lower density of cross-linking with age in [Walters and Eyre, 1983] could have resulted from the use of different tooth types; collagen cross-linking is greatest in molars [Rivera and Yamauchi, 1993]. Clearly, future work addressing the evolution of structure and properties of dentin collagen with aging is essential to understanding its role on the degradation in resistance to fracture of this tissue.

There is presently no clinical approach for arresting cracks in teeth. Thus, preventing crack initiation and growth remains the most viable solution for preventing tooth fracture. Many of the current practices in the field of restorative dentistry are based on knowledge of the structure and properties of the tooth tissues. However, they have not necessarily been developed to accommodate changes in mechanical properties that are associated with aging. Results of this investigation have provided further evidence that aging results in

significant changes in mechanical behavior of dentin, and a reduction in the “damage tolerance” of the tissue. With these findings in mind, the success of specific practices in the field of restorative dentistry may require special consideration in the treatment of seniors, or the development of age-sensitive methods of care.

CONCLUSIONS

An experimental evaluation on the crack growth resistance of human coronal dentin was conducted using tissue obtained from patients between 18 and 83 years of age and for crack extension oriented perpendicular to the dentin tubules. Results of the investigation distinguished that:

1. Dentin undergoes an increase in the resistance to fracture with crack extension (i.e. rising R-curve behavior). For the young dentin ($18 \leq \text{age} \leq 35$) the average resistance to crack growth was characterized in terms of an initiation ($K_o = 1.34 \text{ MPa} \cdot \text{m}^{0.5}$), growth ($K_g = 0.93 \text{ MPa} \cdot \text{m}^{0.5}/\text{mm}$) and plateau toughness ($K_p = 1.65 \text{ MPa} \cdot \text{m}^{0.5}$). For the old dentin ($55 \leq \text{age}$), the initiation ($K_o = 1.08 \text{ MPa} \cdot \text{m}^{0.5}$), and plateau toughness ($K_p = 1.17 \text{ MPa} \cdot \text{m}^{0.5}$) were significantly ($p \leq 0.0001$) less than those values obtained for young dentin.
2. The degree of toughening with crack extension in human dentin is the lowest for crack growth oriented perpendicular to the tubules, regardless of age. Though the toughness of dentin appears to decrease with age regardless of tubule orientation, the degree of anisotropy in resistance to fracture does not.
3. For crack extension in dentin directed perpendicular to the axis and plane of the tubules, toughening is achieved primarily by extrinsic mechanisms and results from bridging forces posed by collagen fibrils and unbroken ligaments spanning the crack. The reduction in toughness with aging in this orientation results from a decrease in number of unbroken ligaments and a reduction in their strength.

Acknowledgments

This work was supported in part by the National Science Foundation through award BES 0238237 and by the National Institute of Dental and Craniofacial Research through award DE 016904. The author A. Nazari wishes to acknowledge his support from a GAANN Fellowship awarded to UMBC. The author D. Zhang would like to thank the Education Committee of Shanghai for supporting his efforts through Grant # 04AB59.

Footnotes

¹The “growth” toughness was defined as the increase or “slope” in resistance to crack growth per unit crack extension.

²SMZ-800 Steromicroscope; Nikon, Tokyo, Japan

³CV-A1 CCD camera; JAI America Inc., Laguna Hills, CA

⁴The “degree of anisotropy” is defined here to indicate the ratio in resistance to failure (in terms of the critical stress or toughness) between two different tubule orientations.

References

1. United States Department of Commerce, Bureau of the Census, 1996. Population projections of the United States by Age, Sex, Race and Hispanic Origin: 1995 to 2050, Current Population Reports No. P25–1130, Washington, DC.

2. Ager JW, 3rd, Nalla RK, Balooch G, Kim G, Pugach M, Habelitz S, Marshall GW, Kinney JH, Ritchie RO. On the increasing fragility of human teeth with age: a deep-UV resonance Raman study. *J Bone Miner Res*. 2006;21:1879–1887. [[PubMed](#)] [[Google Scholar](#)]
3. Anderson TL. *Fracture Mechanics: Fundamentals and Applications*. 3. Boca Raton, FL: CRC Press; 2004. [[Google Scholar](#)]
4. Arola D, Rouland JA, Zhang D. Fatigue and fracture of bovine dentin. *Exp Mech*. 2002;42:380–388. [[Google Scholar](#)]
5. Arola D, Reprogl RK. Effects of aging on the mechanical behavior of human dentin. *Biomaterials*. 2005;26:4051–4061. [[PubMed](#)] [[Google Scholar](#)]
6. Arola D, Reprogl RK. Tubule orientation and the fatigue strength of human dentin. *Biomaterials*. 2006;27:2131–2140. [[PubMed](#)] [[Google Scholar](#)]
7. Arola D. Fracture and Aging in Dentin. In: Curtis RV, Watson TF, editors. *Dental Biomaterials: Imaging, Testing and Modeling*. Woodhead Publishing; Cambridge, UK: 2007. [[Google Scholar](#)]
8. Arola D, Reid J, Cox ME, Bajaj D, Sundaram N, Romberg E. Transition behavior in fatigue of human dentin: structure and anisotropy. *Biomaterials*. 2007;28:3867–3875. [[PubMed](#)] [[Google Scholar](#)]
9. Bajaj D, Sundaram N, Nazari A, Arola D. Age, dehydration and fatigue crack growth in dentin. *Biomaterials*. 2006;27:2507–2517. [[PubMed](#)] [[Google Scholar](#)]
10. Bajaj D, Sundaram N, Arola D. An examination of fatigue striations in human dentin: In vitro and in vivo. *J Biomed Mater Res: Appl Biomater*. 2008;85:149–159. [[PubMed](#)] [[Google Scholar](#)]
11. Carrigan P, Morse DR, Furst MS, Sinai IH. A scanning electron microscope evaluation of human dentin tubules according to age and location. *J Endo*. 1984;10:359–363. [[PubMed](#)] [[Google Scholar](#)]
12. Currey JD, Brear K, Zioupos P. The effects of ageing and changes in mineral content in degrading the toughness of human femora. *J Biomech*. 1996;29:257–260. [[PubMed](#)] [[Google Scholar](#)]
13. Currey JD. *Bones: Structure and Mechanics*. Princeton University Press; Princeton, NJ: 2006. [[Google Scholar](#)]
14. Elwood TW. The future of health care in the United States. *Int Q Community Health Educ*. 2007;26:5–21. [[PubMed](#)] [[Google Scholar](#)]
15. Garrett N, Martini EM. The boomers are coming: a total cost of care model of the impact of population aging on the cost of chronic conditions in the United States. *Dis Manag*. 2007;10:51–60. [[PubMed](#)] [[Google Scholar](#)]
16. Imbeni V, Nalla RK, Bosi C, Kinney JH, Ritchie RO. In vitro fracture toughness of human dentin. *J Biomed Mater Res A*. 2003;66:1–9. [[PubMed](#)] [[Google Scholar](#)]
17. Iwamoto N, Ruse ND. Fracture toughness of human dentin. *J Biomed Mater Res A*. 2003;66:507–512. [[PubMed](#)] [[Google Scholar](#)]
18. Kahler B, Swain MV, Moule A. Fracture-toughening mechanisms responsible for differences in work to fracture of hydrated and dehydrated dentine. *J Biomech*. 2003;36:229–237. [[PubMed](#)] [[Google Scholar](#)]
19. Kinney JH, Nalla RK, Pople JA, Breunig TM, Ritchie RO. Age-related transparent root dentin: mineral concentration, crystallite size, and mechanical properties. *Biomaterials*. 2005;26:3363–3376. [[PubMed](#)] [[Google Scholar](#)]
20. Koester KJ, Ager JW, 3rd, Ritchie RO. The effect of aging on crack-growth resistance and toughening mechanisms in human dentin. *Biomaterials*. 2008;29:1318–1328. [[PubMed](#)] [[Google Scholar](#)]
21. Kruzic JJ, Nalla RK, Kinney JH, Ritchie RO. Crack blunting, crack bridging and resistance-curve fracture mechanics in dentin: effect of hydration. *Biomaterials*. 2003;24:5209–5221. [[PubMed](#)] [[Google Scholar](#)]
22. Malik CL, Stover SM, Martin RB, Gibeling JC. Equine cortical bone exhibits rising R-curve fracture mechanics. *J Biomech*. 2003;36:191–198. [[PubMed](#)] [[Google Scholar](#)]
23. Mjör IA, Nordahl I. The density and branching of dentinal tubules in human teeth. *Arch Oral Biol*. 1996;41:401–412. [[PubMed](#)] [[Google Scholar](#)]

24. Nalla RK, Kinney JH, Ritchie RO. Effect of orientation on the in vitro fracture toughness of dentin: the role of toughening mechanisms. *Biomaterials*. 2003;24:3955–3968. [[PubMed](#)] [[Google Scholar](#)]
25. Nalla RK, Kruzic JJ, Kinney JH, Ritchie RO. Effect of aging on the toughness of human cortical bone: evaluation by R-curves. *Bone*. 2004;35:1240–1246. [[PubMed](#)] [[Google Scholar](#)]
26. Nalla RK, Porter AE, Daraio C, Minor AM, Radmilovic V, Stach EA, Tomsia AP, Ritchie RO. Ultrastructural examination of dentin using focused ion-beam cross-sectioning and transmission electron microscopy. *Micron*. 2005b;36:672–680. [[PubMed](#)] [[Google Scholar](#)]
27. Nalla RK, Kruzic JJ, Kinney JH, Ritchie RO. Mechanistic aspects of fracture and R-curve behavior in human cortical bone. *Biomaterials*. 2005b;26:217–231. [[PubMed](#)] [[Google Scholar](#)]
28. Nalla RK, Kinney JH, Tomsia AP, Ritchie RO. Role of alcohol in the fracture resistance of teeth. *J Dent Res*. 2006;85:1022–1026. [[PMC free article](#)] [[PubMed](#)] [[Google Scholar](#)]
29. Porter AE, Nalla RK, Minor A, Jinschek JR, Kisielowski C, Radmilovic V, Kinney JH, Tomsia AP, Ritchie RO. A transmission electron microscopy study of mineralization in age-induced transparent dentin. *Biomaterials*. 2005;26:7650–7660. [[PubMed](#)] [[Google Scholar](#)]
30. Rivera EM, Yamauchi M. Site comparisons of dentine collagen cross-links from extracted human teeth. *Arch Oral Biol*. 1993;38:541–546. [[PubMed](#)] [[Google Scholar](#)]
31. Schilke R, Lisson JA, Bauss O, Geurtsen W. Comparison of the number and diameter of dentinal tubules in human and bovine dentine by scanning electron microscopic investigation. *Arch Oral Biol*. 2000;45:355–361. [[PubMed](#)] [[Google Scholar](#)]
32. Ten Cate AR. *Oral Histology: Development, Structure, and Function*. 5. Mosby-Year Book, Inc; St. Louis: 1998. [[Google Scholar](#)]
33. Thompson DD. Age changes in bone mineralization, cortical thickness, and haversian canal area. *Calcif Tissue Int*. 1980;31:5–11. [[PubMed](#)] [[Google Scholar](#)]
34. Ural A, Vashishth D. Cohesive finite element modeling of age-related toughness loss in human cortical bone. *J Biomech*. 2006;39:2974–2982. [[PubMed](#)] [[Google Scholar](#)]
35. Ural A, Vashishth D. Anisotropy of age-related toughness loss in human cortical bone: a finite element study. *J Biomech*. 2007;40:1606–1614. [[PubMed](#)] [[Google Scholar](#)]
36. Vasiliadis L, Darlin AI, Levers BG. The histology of sclerotic human root dentine. *Arch Oral Biol*. 1983;28:693–700. [[PubMed](#)] [[Google Scholar](#)]
37. Walters C, Eyre DR. Collagen crosslinks in human dentin: increasing content of hydroxypyridinium residues with age. *Calcif Tissue Int*. 1983;35:401–405. [[PubMed](#)] [[Google Scholar](#)]
38. Wang X, Shen X, Li X, Agrawal CM. Age-related changes in the collagen network and toughness of bone. *Bone*. 2002;31:1–7. [[PubMed](#)] [[Google Scholar](#)]
39. Wang X, Puram S. The toughness of cortical bone and its relationship with age. *Ann Biomed Eng*. 2004;32:123–135. [[PubMed](#)] [[Google Scholar](#)]
40. Weber DF. Human dentine sclerosis: A microradiographic survey. *Arch Oral Biol*. 1974;19:163–169. [[PubMed](#)] [[Google Scholar](#)]
41. Zhang D, Arola D. Application of digital image correlation to biological tissues. *J Biomed Opt*. 2004;9:691–699. [[PubMed](#)] [[Google Scholar](#)]
42. Zhang D, Luo M, Arola D. Displacement/strain measurement under optical microscope with digital image correlation. *Opt Engr*. 2006;45:1–9. [[Google Scholar](#)]
43. Zhang D, Nazari A, Soappman M, Bajaj D, Arola D. Methods for examining the fatigue and fracture behavior of hard tissues. *Exp Mech*. 2007;47:325–336. [[Google Scholar](#)]
44. Zioupos P, Currey JD. Changes in the stiffness, strength, and toughness of human cortical bone with age. *Bone*. 1998;22:57–66. [[PubMed](#)] [[Google Scholar](#)]
45. Zioupos P, Currey JD, Hamer AJ. The role of collagen in the declining mechanical properties of aging human cortical bone. *J Biomed Mater Res*. 1999;45:108–116. [[PubMed](#)] [[Google Scholar](#)]